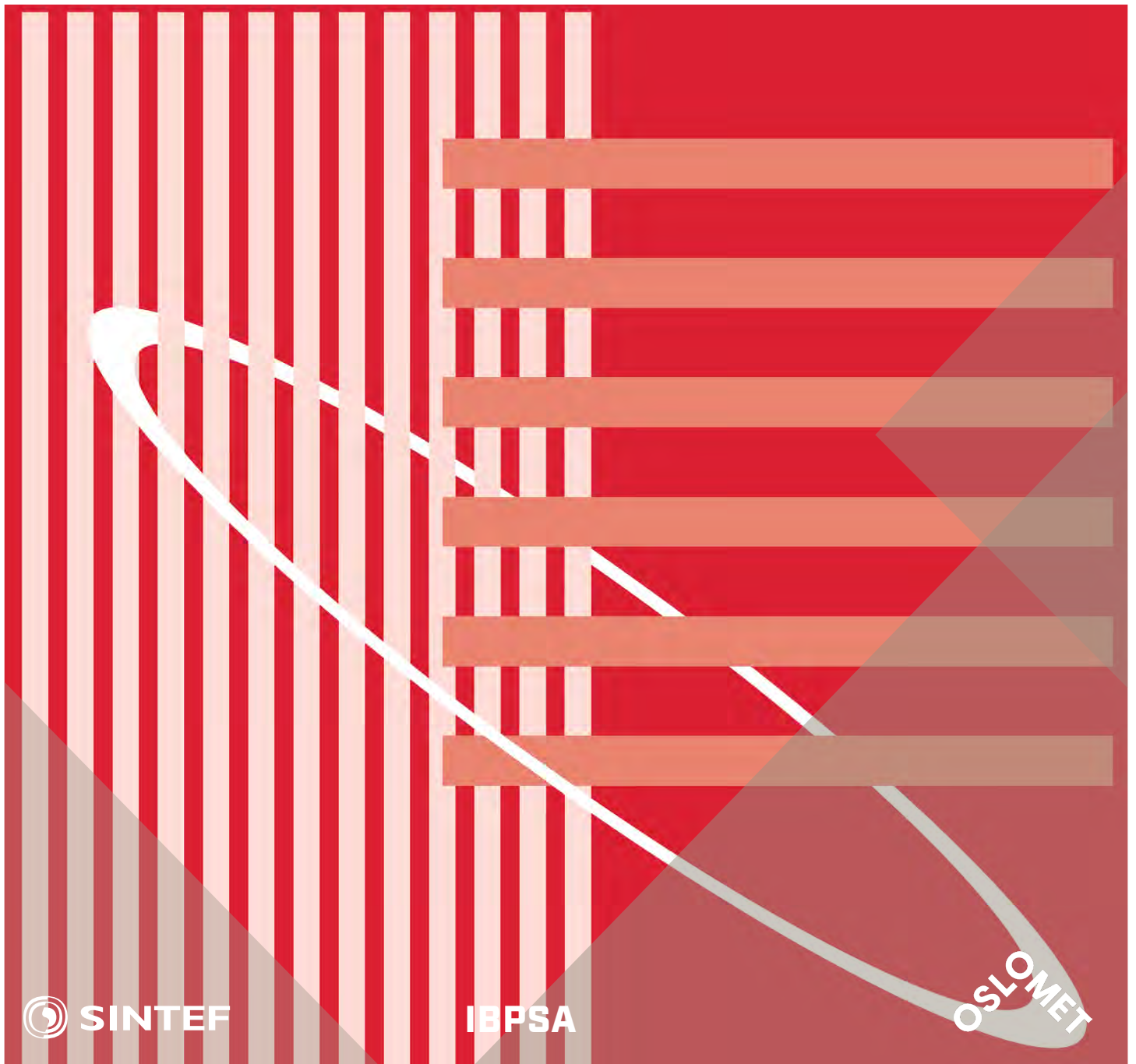


International Conference Organised by
IBPSA-Nordic, 13th-14th October 2020,
OsloMet

BuildSIM-Nordic 2020

Selected papers



SINTEF Proceedings

Editors:

Laurent Georges, Matthias Haase, Vojislav Novakovic and Peter G. Schild

BuildSIM-Nordic 2020

Selected papers

International Conference Organised by IBPSA-Nordic,
13th–14th October 2020, OsloMet

SINTEF Academic Press

SINTEF Proceedings no 5

Editors:

Laurent Georges, Matthias Haase, Vojislav Novakovic and Peter G. Schild

BuildSIM-Nordic 2020

Selected papers

International Conference Organised by IBPSA-Nordic,

13th–14th October 2020, OsloMet

Keywords:

Building acoustics, Building Information Modelling (BIM), Building physics, CFD and air flow, Commissioning and control, Daylighting and lighting, Developments in simulation, Education in building performance simulation, Energy storage, Heating, Ventilation and Air Conditioning (HVAC), Human behavior in simulation, Indoor Environmental Quality (IEQ), New software developments, Optimization, Simulation at urban scale, Simulation to support regulations, Simulation vs reality, Solar energy systems, Validation, calibration and uncertainty, Weather data & Climate adaptation, Fenestration (windows & shading), Zero Energy Buildings (ZEB), Emissions and Life Cycle Analysis

Cover illustration: IBPSA-logo

ISSN 2387-4295 (online)

ISBN 978-82-536-1679-7 (pdf)



© The authors

Published by SINTEF Academic Press 2020

This is an open access publication under the CC BY-NC-ND license

(<http://creativecommons.org/licenses/by-nc-nd/4.0/>).

SINTEF Academic Press

Address: Børrestuveien 3

PO Box 124 Blindern

N-0314 OSLO

Tel: +47 40 00 51 00

www.sintef.no/community

www.sintefbok.no

SINTEF Proceedings

SINTEF Proceedings is a serial publication for peer-reviewed conference proceedings on a variety of scientific topics.

The processes of peer-reviewing of papers published in SINTEF Proceedings are administered by the conference organizers and proceedings editors. Detailed procedures will vary according to custom and practice in each scientific community.

A novel modelling approach of ground source heat pump application for district heating and cooling, developed for a case study of an urban district in Finland

Oleg Todorov^{1*}, Kari Alanne¹, Markku Virtanen¹, Risto Kosonen^{1,2}

¹Aalto University, Helsinki, Finland

²Nanjing Tech University, Nanjing, China

* *corresponding author: oleg.todorovradoslavov@aalto.fi*

Abstract

The world impact of fossil fuels on air pollution is responsible for several millions premature deaths every year. The present study analyses the decarbonization of district heating (DH) and cooling (DC) networks by the integration of ground source heat pump (GSHP) within an urban district in southwestern Finland, in terms of technoeconomic feasibility, efficiency and environmental impact. A novel mathematical modelling for GSHP operation and energy system management is proposed and demonstrated, using hourly-based data for heating and cooling demand. Hydrogeological and geographic data from different Finnish data sources is retrieved in order to calibrate and validate a groundwater model. Three different Scenarios for GSHP operation are investigated, limited by the maximum pumping flow rate of the groundwater area. The additional pre-cooling exchanger in Scenario 2 and 3 resulted in an important advantage, since it increased the heating and cooling demand covered by GSHP by 15% and 16% respectively as well as decreased the energy production cost by 4%. Moreover, Scenario 3 was solved as nonlinear optimization problem resulting in 4% lower pumping rate compared to Scenario 2. Overall, the annually balanced GSHP management in terms of energy and pumping flows, resulted in low long-term environmental impact and is economically feasible (energy production cost below 30 €/MWh).

Introduction

Worldwide, some 4.5 million people die prematurely every year due to air pollution generated by burning fossil fuels and the increased levels of PM_{2.5}, while the overall cost is estimated as 3.3% of world GDP (Greenpeace 2020). Recent study also relates the mortality of Covid-19 and the long-term exposure to air pollution and PM_{2.5}, concluding that small increase in PM_{2.5} exposure has 20 times more lethal impact in Covid-19 death rate (Wu et al. 2020). Therefore, a decarbonization of our existing energy networks, based primarily on fossil fuels generation, is a necessity for sustainable and healthy future. According to Eurostat, in 2018 the share of renewable energy sources (RES) used for heating and cooling in the European Union was 21% and several countries like Sweden (65%), Latvia (56%), Finland (55%) and Estonia (54%) covered more than half of their

heating and cooling consumption with renewables sources (Eurostat 2020). The variability of renewable generation between heating and cooling seasons, as well as the low coincidence between supply and demand are important challenges for RES penetration, therefore short- and long-term energy storage is needed for maximizing the usage of RES.

Wherever the hydrogeological conditions are favourable, Aquifer Thermal Energy Storage (ATES) is an attractive technological option, suitable for large buildings and utilities (Fleuchaus et al. 2018) as well as capable to enable important thermal storage capacities (Pellegrini et al. 2019). Fleuchaus et al. (2018) presented a complete overview of global ATES development and application: some 3000 ATES systems are operated nowadays worldwide. The Netherlands with 85% of all ATES realizations, followed by Sweden, Denmark and Belgium, are the undisputed frontrunners. From these 3000 ATES applications worldwide, there are some 100 large-scale utility systems, integrated in DH/DC networks (Schmidt et al. 2018).

In the same line, ground-source heat pump (GSHP) is a key technology for a decarbonization of the existing heating and cooling, nowadays mostly based on the utilization of fossil fuels (Paiho et al. 2018; Soltani et al. 2019; Popovski et al. 2019). The work of Paiho et al. 2018 revealed that large-scale heat pumps are crucial for increasing the flexibility of the Finnish energy systems. Within the same research, different examples are presented for heat pump integration in Finnish DH/DC networks: in Turku - the Kakola plant recycling heat from sewage wastewater, and in Helsinki - the Katri Vala plant generating heating and cooling in a single process. Fleuchaus et al. (2019) evaluated the performance of ATES based on different criteria and concluded that ATES integration into heating and cooling systems were rarely addressed. In order to fill this gap, the integration of GSHP in tandem with ATES within the existing DH/DC networks of a Finnish urban district, is presented and developed in the current case study.

The novelty of the present research is to introduce a mathematical modelling of the whole energy chain ATES-GSHP-DH-DC in order to improve system's energy management, as well as to study its technical

justification, economic feasibility and the long-term impact of GSHP-ATES operation. Finnish public data sources are available, like the Finnish Environmental Institute (SYKE) regarding the hydrological resources; Geological Survey of Finland (GTK) - hydrogeological conditions, and the National Land Survey of Finland (NLSF) for geographical data. The present research also presents a methodology for fetching data from the aforementioned sources for calibrating and validating a groundwater model, which in turn is an essential tool for studying the long-term impact on the aquifer area.

Methods

The modelling procedure of the combined ATES-GSHP-DH-DC system is based on the following steps, namely - i) input data of the target DH/DC networks and the nearby groundwater areas, ii) mathematical modelling of combined ATES-GSHP operation, iii) techno-economic analysis, and iv) impact of ATES-GSHP operation on aquifer areas, by developing and calibrating a specific groundwater model. Groundwater model based on the finite-difference-method software MODFLOW (Harbaugh et al. 2005) is developed in this case study, which is calibrated against long-term data (hydraulic heads of the observation wells) of the studied aquifer.

Input data for GSHP integration

Input data of the DH and DC networks

The target DH/DC networks are located in the central district of Kupittaa in the town of Turku, located in the south-west part of Finland. The available data is hourly-based and the most relevant parameters of both DH and DC networks are summarized in *Table 1* and *Figure 1*.

Table 1. Relevant DH / DC network parameters

Network parameters	DH network	DC network
Annual energy demand, MWh	67,971	12,382
Max./min. load, MW	27.06 / 0.43	6.38 / 0.52
Avg. load (\pm stand. dev.), MW	7.76 \pm 4.8	1.41 \pm 0.7
Max./min. supply temp., °C	110.4 / 56.0	10.0 / 5.3
Avg. supply temperature, °C	84.3 \pm 7.8	6.6 \pm 0.3
Max./min. return temp., °C	51.4 / 22.7	14.8 / 10.0
Avg. return temperature, °C	40.9 \pm 2.8	13.5 \pm 0.4

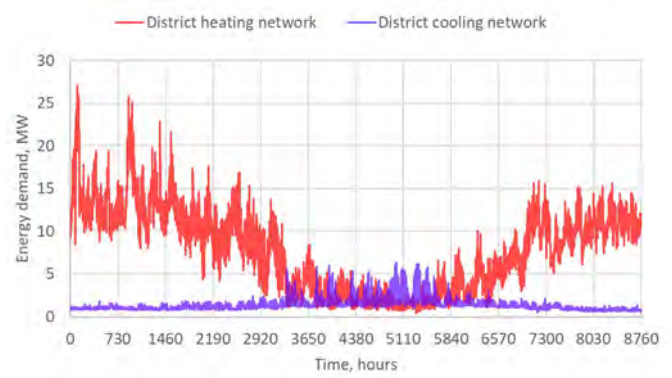


Figure 1. Annual energy demand of DH / DC networks

Input data for a groundwater model

The impact of GSHP-ATES operation is studied by developing a generic groundwater model. Typical data for an esker aquifer located in southwestern Finland is utilized, relative to groundwater areas, monitoring stations and observation wells. Additionally, open data from the National Land Survey of Finland is used, particularly its "10m elevation model". The elevation model is retrieved as Geo-TIFF raster file, transformed to Surfer Grid file (GRD) using QGIS (QGIS, 2019).

GSHP-ATES utilization for DH/DC

Ground-source heat pump (GSHP), operating with groundwater open-loop *well doublet* (comprising groundwater abstraction and injection wells), is considered. The condenser side of the heat pump is connected to DH network while the evaporator side is connected to aquifer pumping stream. Three different scenarios have been investigated. In the first Scenario, the ATES pumping flow path encounters two serial exchangers – HP evaporator and cooling for DC network. In Scenario 2 and 3, a pre-cooling exchanger is added before the HP evaporator, providing 1st stage cooling to the DC network.

As will be shown in the result section, with this configuration the DC demand can be more efficiently covered and HP efficiency (COP) is improved since heat pump inlet temperature increases several degrees after a pre-cooling exchanger. GSHP-ATES integration within existing DH/DC networks is depicted in the general scheme presented in *Figure 2*, where temperature values illustrate the setup of Scenario 2/3.

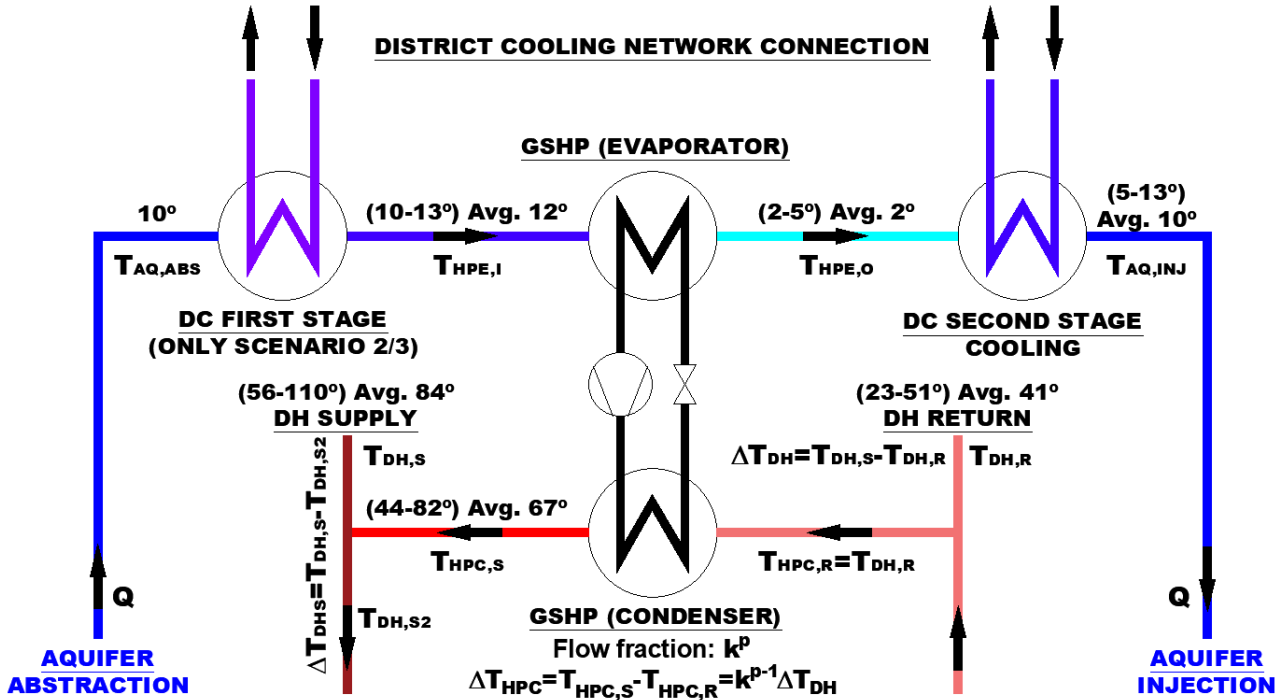


Figure 2. General scheme of GSHP-ATES integration

Modelling tools and methods

GSHP utilization for district heating

GSHP is used to recover and upgrade all excess heat proceeding from the DC network and inject it in DH network. In this context ATES is utilized for balancing the energy system and mitigating the variability and non-coincidence of the simultaneously dispatched heating and cooling loads. To that end, heat pump supply temperature is calculated, based on the demanded power fraction k (the ratio between heat supplied by the heat pump and total heat demanded in the DH branch). The flow fraction recirculated through HP condenser can be calculated as: k^p , where $0 \leq p \leq 1$ is additional exponent parameter. For each hour n , given that $T_{DH,R,n}$ and $T_{DH,S,n}$ are DH return and supply temperatures respectively, the heat pump supply temperature $T_{HPC,S,n}$ can be calculated as follows:

$$T_{HPC,S,n} = T_{DH,R,n} + (T_{DH,S,n} - T_{DH,R,n})k^{1-p} \\ \Rightarrow \Delta T_{HPC,n} = \Delta T_{DH,n}k^{1-p} \quad (1)$$

And the resulted supply temperature $T_{DH,S2,n}$ after mixing can be computed as:

$$T_{DH,S2,n} = T_{DH,S,n} + (T_{DH,S,n} - T_{DH,R,n})(k - k^p) \\ \Rightarrow \Delta T_{DHS,n} = T_{DH,S,n} - T_{DH,S2,n} = \Delta T_{DH,n}(k^p - k) \quad (2)$$

The parameter p is chosen equal to 0.6, which can be advantageous in partial load operation. For example, for power fraction $k = 0.4$ and $\Delta T_{DH} = 40^\circ\text{C}$, GSHP should elevate DH return temperature by roughly 28°C instead of 40°C . After mixing with supply DH flow, the temperature drop ΔT_{DHS} is around 7°C .

COP_H estimation model

According to Reinholdt (2018), the maximum theoretical COP of a heat pump can be estimated by calculating Lorentz COP, defined as follows:

$$COP_{Lor} = \frac{T_{lm,H}}{T_{lm,H} - T_{lm,L}}, \text{ where} \\ T_{lm,H} = \frac{T_{HPC,S} - T_{HPC,R}}{\ln\left(\frac{T_{HPC,S}}{T_{HPC,R}}\right)}; T_{lm,L} = \frac{T_{HPE,O} - T_{HPE,I}}{\ln\left(\frac{T_{HPE,O}}{T_{HPE,I}}\right)} \quad (3)$$

In Equation (3), $T_{lm,H}$ and $T_{lm,L}$ are respectively the logarithmic mean temperature of the sink and source, where notations HPC and HPE stand for heat pump's condenser and evaporator temperatures, while notations I/O stand for inlet / outlet temperatures of the evaporator and S/R stand for supply / return temperatures of the condenser (all values expressed in Kelvin). Based on best industrial refrigeration systems, Reinholdt suggested values for Lorentz efficiency between 50 and 60% of the maximum Lorentz COP. In our case study, more conservative value of 45% is adopted.

GSHP utilization for district cooling

As mentioned previously, part of DC demand can be produced by free cooling in a 1st stage cooling exchanger. After that, GSHP is utilized in the second place for simultaneously cooling of ATES flow in the evaporator and supplying heat to DH network in the condenser (see Figure 2). And finally, second stage cooling is applied, and groundwater is injected into the aquifer. For each hour of operation, it is crucial to determine the ATES pumping flow rate Q [m^3/s] since there is constraint for pumping of

2500 m³/day (annual average). Due to this limitation, the max. heat output of GSHP condenser is limited to 1.43/1.67 MW respectively in Scenario 1/2(3) and ATES pumping flow rate is calculated according to the algorithm developed below.

Computation of ATES pumping flow rate

Since in the ATES flow path there are two / three exchangers respectively for Scenario 1/2, the needed pumping flow rate Q can be estimated as follows. For each hour n will be determined whether heating or cooling is dominating, given that $\Phi_{heat,n}$ and $\Phi_{cool,n}$ are respectively heating and cooling demand to be covered (notations according to Figure 2):

- Heating dominates:

$$\text{If } \frac{\left(1 - \frac{1}{COP_n}\right) \Phi_{heat,n}}{S_{VC,wat} (T_{HPE,I,n} - T_{HPE,O,n})} \geq \frac{\Phi_{cool,n}}{S_{VC,wat} (T_{HPE,I,n} - T_{AQ,ABS,n} + T_{AQ,INJ,n} - T_{HPE,O,n})}$$

where $T_{HPE,I,n} = T_{AQ,ABS,n}$ (in SC. 1);

$T_{HPE,I,n} = \max\{T_{AQ,ABS,n}; T_{DC,R,n} - \Delta T_{min}\}$ (in SC. 2);

$T_{AQ,INJ,n,max} = T_{DC,R,n} - \Delta T_{min}$;

$T_{HPE,O,n,min} = 2^\circ C$; $S_{VC,wat} = 4.19 \text{ MJ/m}^3 K$

Where $\Delta T_{min} = 2^\circ C$ is the min. pinch point difference in cooling exchangers and $\Delta T_{HPE,O,n,min} = 2^\circ C$ is the min. temperature after GSHP evaporator. COP_n is calculated with Equation (3), assuming avg. value for $T_{HPE,O} = 2^\circ C$

$$\Rightarrow Q_n = \frac{\left(1 - \frac{1}{COP_n}\right) \Phi_{heat,n}}{S_{VC,wat} (T_{HPE,I,n} - T_{HPE,O,n})}$$

- Cooling dominates (iteration method):

$$\text{If } \frac{\left(1 - \frac{1}{COP_n}\right) \Phi_{heat,n}}{S_{VC,wat} (T_{HPE,I,n} - T_{HPE,O,n})} < \frac{\Phi_{cool,n}}{S_{VC,wat} (T_{HPE,I,n} - T_{AQ,ABS,n} + T_{AQ,INJ,n} - T_{HPE,O,n})}$$

Iteration step: initial Q_n is estimated as

$$S_{VC,wat} (T_{HPE,I,n} - T_{AQ,ABS,n} + T_{AQ,INJ,n} - T_{HPE,O,n})$$

Recalculation of temperature after HP evaporator

$$T_{HPE,O,n} = T_{HPE,I,n} - \frac{\left(1 - \frac{1}{COP_n}\right) \Phi_{heat,n} \cdot Q_n}{S_{VC,wat}}$$

Recalculation of 1st and 2nd stage cooling demands

$$\Phi_{cool-1stage,n} = Q_n S_{VC,wat} (T_{HPE,I,n} - T_{AQ,ABS,n})$$

$$\Phi_{cool-2stage,n} = \min\{Q_n S_{VC,wat} (T_{AQ,INJ,n} - T_{HPE,O,n}); \Phi_{cool,n} - \Phi_{cool-1stage,n}\}$$

$$\Phi_{cool,n} = \Phi_{cool-1stage,n} + \Phi_{cool-2stage,n}$$

The ATES flow is recalculated again in *Iteration step*, taking as new $T_{HPE,O}$ the average of current and previous

value, and if the new Q_n deviates more than a predefined threshold from the previous one (a 5% threshold is adopted), then *Iteration step* is repeated.

Calculation of ATES pumping power demand

The required pumping power [kW] for ATES operation can be calculated in an hourly basis, assuming overall pressure drop in the line $\Delta p = 600 \text{ kPa}$ and standard pumping efficiency $\eta = 0.55$ (Grundfos SP, 2020):

$$P_{ATES,n} = \frac{Q_n \Delta p}{\eta} \quad (4)$$

Calculation of pumping power demand to DH/DC

Similarly, pumping power [kW] to provide DH/DC through GSHP condenser / evaporator respectively can be calculated in an hourly-basis, assuming overall pressure drop between supply and return lines $\Delta p_{DH} = \Delta p_{DC} = 250 \text{ kPa}$ (DH 2008) and standard pumping efficiency $\eta = 0.55$ (Grundfos NB/NBG, 2020), as follows:

$$P_{HPC-DH,n} = \frac{Q_{HPC,n} \Delta p_{DH}}{\eta}; P_{HPE-DC,n} = \frac{Q_{HPE,n} \Delta p_{DC}}{\eta} \quad (5)$$

$$\text{where } Q_{HPC,n} = \frac{\Phi_{supplied-heat,n}}{S_{VC,wat} (T_{HPC,S,n} - T_{DH,R,n})}; Q_{HPE,n} = \frac{\Phi_{cool-1stage,n} + \Phi_{cool-2stage,n}}{S_{VC,wat} (T_{DC,R,n} - T_{DC,S,n})}$$

The volumetric heat capacity of water $S_{VC,wat}$ used is 4.19 and 4.1 MJ/m³K respectively for cooling and heating.

Calculation of ATES pumping rate using nonlinear optimization techniques

It is possible to solve ATES pumping flow rate Q_n setting up an optimization problem for each hour of operation. Both Q_n and specific energy consumption of GSHP compressor and ATES pumping need to be minimized. Additional nonlinear optimization problem (Scenario 3) is set up for Scenario 2, defined as follows:

$$\text{Objective function: } \min \left(Q_n + \frac{P_{ATES,n} + P_{HPC,n}}{\Phi_{heat,n} + \Phi_{cool,n}} \right)$$

$$\text{where } P_{ATES,n} = \frac{Q_n \Delta p}{\eta} \text{ (eq. 4) and } P_{HPC,n} = \frac{\Phi_{heat,n}}{COP_n};$$

$$\Phi_{cool,n} = \Phi_{cool-1stage,n} + \Phi_{cool-2stage,n}$$

$$\Phi_{cool-1stage,n} = Q_n S_{VC,wat} (T_{HPE,I,n} - T_{AQ,ABS,n})$$

$$\Phi_{cool-2stage,n} = \min\{Q_n S_{VC,wat} (T_{AQ,INJ,n} - T_{HPE,O,n}); \Phi_{cool,n} - \Phi_{cool-1stage,n}\}$$

Subject to constraints: $0.01 \leq Q_n \leq 0.05 \text{ [m}^3/\text{s]}$

$$T_{HPE,O,n} \geq 2; T_{AQ,INJ,n} \leq T_{DC,R,n} - 2$$

The model is solved for each hour by varying Q_n and using GRG nonlinear solver in MS Excel.

Numerical model and steady state calibration

MODFLOW (Harbaugh et al. 2005) as finite difference code, under ModelMuse environment (ModelMuse, 2019) is used for the groundwater model. The

discretization of the aquifer area is done using 100x100 m square cell grid, covering a physical extension of about 20 km². Available information is used for 15 close-field observation wells and 8 far-field wells, and their long-term statistical data (average head) in order to calibrate the groundwater model for steady state (see *Figure 3*). The average aquifer thickness is estimated as 10 m (Joronen, 2009) and the maximum allowed average pumping rate is 2500 m³/day (Arola et al. 2014).

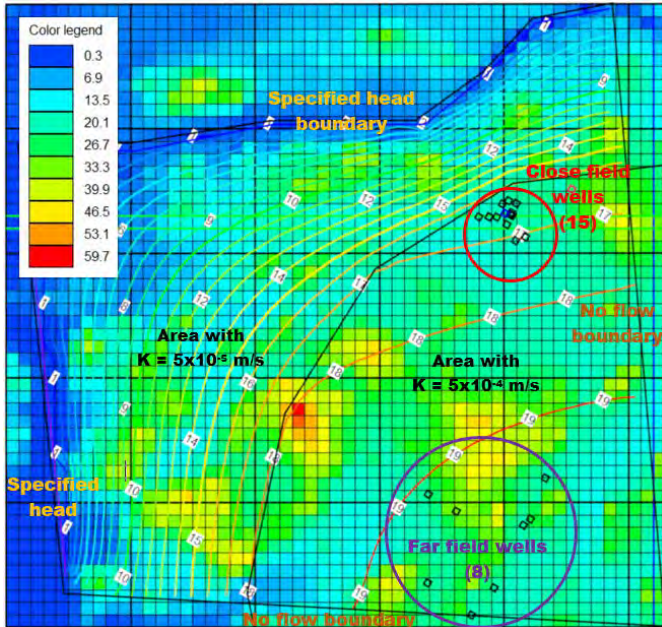


Figure 3. Numerical model and steady state solution

The undisturbed aquifer temperature in Kupittaa area is around 10°C (Arola et al. 2014), quite high due to the subsurface heat island effect (Bayer et al. 2019) observed in high density urban areas like Kupittaa, composed mostly by educational and healthcare buildings, sport facilities and dwellings. North-west and south-west are set as specified head boundaries, while south-east and north-east borders are assumed as no-flow boundaries

Groundwater model calibration for steady state is done according to the procedure developed by Todorov et al. (2020a), and results with RMSE for close- and far-field areas are presented in *Figure 4*, where bubbles' diameter is the standard deviation of the measured values. A steady state solution is shown in *Figure 3*, where iso-lines are hydraulic heads while color legend represents elevations (in meters above sea level).

A typical horizontal hydraulic conductivity for sand/gravel aquifer is selected: $K=5 \times 10^{-5}$ m/s (Luoma 2018), and during model calibration is adjusted to 5×10^{-4} m/s for the area containing the observation wells. Vertical hydraulic conductivity K_z is assigned equal to $0.1K$. Typical values are also utilized for storativity ($S=1 \times 10^{-5}$ m/s), porosity ($n = 0.25$) and recharge rate of $R=1.3 \times 10^{-8}$ m/s (Luoma 2018).

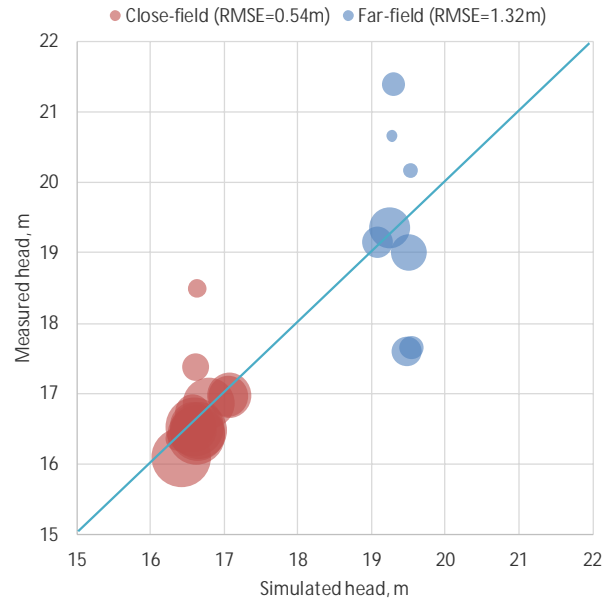


Figure 4. Groundwater model calibration

Technoeconomic evaluation of GSHP-ATES

Based on hourly calculations, different technical variables are computed, like the annual energy demand for heating, cooling and electricity as well as the average daily ATES pumping rate. Cost database regarding various energy generation technologies is used (after Nielsen et al. 2013; DAE 2020), as well as prices for ATES well drilling, heat exchangers and piping (Drenkelfort et al. 2015) for estimating the investment cost. Based on the annuity method, energy generation cost is calculated, assigning annual investment payments (annuity) and assuming 20 years investment's lifetime (Nielsen et al., 2013) / interest rate of 5%. O&M costs (1% of overall investment cost) and electricity cost for GSHP and pumping, given electricity price of 100€/MWh (with taxes, transfer and distribution fees, Nordpool 2020), are also included within the overall annual cost. The economic evaluation is done after Todorov et al. (2020b), and it comprises the calculation of the following variables shown in *Table 2*.

Table 2. Variables for economic evaluation

Variable	Units	Comments
Overall investment cost	€	Geological survey, GSHP, exchangers, drilling and piping
Annuity factor	-	Computed for 20 years lifetime and 5% interest rate
Investment cost (annuity)	€	Overall investment cost times the annuity factor
O&M costs	€	1% of overall investment cost
Annual electricity cost	€	Cost of electricity demand (GSHP and pumping)
Overall annual cost	€	Annuity + O&M costs + energy cost
Specific energy cost	€/MWh	Overall annual cost per total thermal energy generation

Results and discussion

Technoeconomic analysis

The main technical variables of ATES-GSHP operation for all studied scenarios are presented in *Table 3*. It can be seen, that even with 5-6% of peak heat power respectively for Scenario 1-2/3, the GSHP coverage ratio is 18-21% of the annual heating demand. Moreover, an important advantage of Scenario 2/3 is shown when comparing a cooling demand covered by GSHP. The scheme with two cooling exchangers in Scenario 2 allows to cover 78% of DC demand annually (compared to 67% in Scenario 1), from which the 1st stage cooling accounts for roughly 1/6. The investment cost estimation of ATES-GSHP system as well as the cost of generated thermal energy are presented in *Table 4* and *Table 5* respectively.

Table 3. Technical variables of ATES-GSHP system

Annual results for Scenario 1/2/3	Sc. 1	Sc. 2	Sc. 3
Peak pre-cooling/heating/cooling power, MW	-1.43/1	0.3/1.67/1.2	
Avg. ATES pumping rate, m ³ /day	2478	2487	2393
Avg. abstraction temperature, °C	10.0	10.0	
Avg. injection temperature, °C	10.0	10.0	
Avg. temperature before GSHP, °C	10.0	11.5	
Avg. temperature after GSHP, °C	2.1	2.4	2.0
Avg. HP supply temperature, °C	65.4	66.7	
Avg. DH return temperature, °C	40.9	40.9	
Avg. GSHP COP (heating mode)	3.14	3.15	
Heating demand (DH), MWh	67,971		
Heat demand covered, MWh	12,315	14,189	
Heat demand covered by GSHP, %	18 %	21 %	
Cooling demand (DC), MWh	12,382		
1 st stage cooling covered, MWh	-	1,604	1,548
2 nd stage cooling covered, MWh	8,323	8,031	8,031
Total cooling demand, MWh	8,323	9,635	9,578
Total cooling demand covered, %	67 %	78 %	77 %
Electricity demand (GSHP), MWh	3,934.2	4,509.3	4,509.3
Elec. demand (ATES), MWh	274.1	275.0	264.7
Elec. demand (HP- DH), MWh	57.7	63.0	63.0
Elec. demand (HP- DC), MWh	130.6	150.9	150.0
Total electricity demand, MWh	4,396.6	4,998.2	4,987.0

Table 4. Investment cost of ATES-GSHP system

Investment cost	Price	Total Sc. 1	Total Sc. 2/3
Subsurface study, geological report and pumping tests, €	30,000	30,000	
GS heat pump, €/kW	300	429,000	501,000
Heat exchangers, €/kW	35	85,050	110,950
Pumping well (including equipment and pump), €/u	170,000	1,360,000	
PEHD connection pipes, €/m	250	325,000	
Overall investment cost, €		2,229,050	2,326,950

The resulted thermal energy production cost in Scenario 2 and 3 is slightly below 30 €/MWh. Overall investment cost is around 2.3 million €; 26% of the investment account for GSHP / exchangers and 72% is related to the underground components (connection pipes and wells), figures close to similar ATES realization in Germany (Schüppler et al. 2019).

The optimized Scenario 3 has slightly higher energy production cost (+0.1%) compared to Scenario 2 (*Table 5*), however, there is an important -4% reduction of the average ATES pumping rate (*Table 3*). The average COP is not significantly improved from Scenario 1 to Scenario 2/3, even though evaporator's entering temperature is 1.5 °C higher on average. This is due to the higher heat fraction which increases the average HP production temperature from 65 to 67 °C on average.

Table 5. Energy production cost

Annuity method	Sc.1	Sc.2	Sc.3
Annuity factor (5% / 20 years)	0.0802		
Annual investment cost, €	178,865	186,720	186,720
Annual fixed O&M cost, €	22,291	23,270	23,270
Annual energy cost (elec.), €	439,663	499,819	498,699
Total annual cost, €	640,818	709,809	708,689
Cost per MWh of energy, €	31.05	29.79	29.82

GSHP operation is based on energy conversion using electricity to co-generate heating and cooling in a single process. GSHP is the main electricity consumer accounting for 90% of the annual demand, followed by ATES pumping (6%) as well as pumping needed to inject HP's supply energy to DH/DC networks – respectively 1% / 3%. This is important to be acknowledged since total electricity demand (some 5 GWh/a in Scenario 2 and 3) has a significant impact on the annual cost and, consequently on the specific cost of generated heating and cooling energy, as can be seen in *Table 5*.

ATES system is well balanced, as seen from the average injection and abstraction temperatures equal both to aquifer's undisturbed temperature of 10 °C. Moreover, the system is balanced in terms of energy, as shown in *Table 3*, since the annual heat demand covered is equal to cooling demand covered plus GSHP power demand (around 12.3 and 14.2 GWh in Scenario 1 and 2/3 respectively).

The annual variation of all temperatures along ATES flow path in Scenario 2: abstraction, after 1st stage cooling, after GSHP evaporator and finally injection, is shown in *Figure 5*.

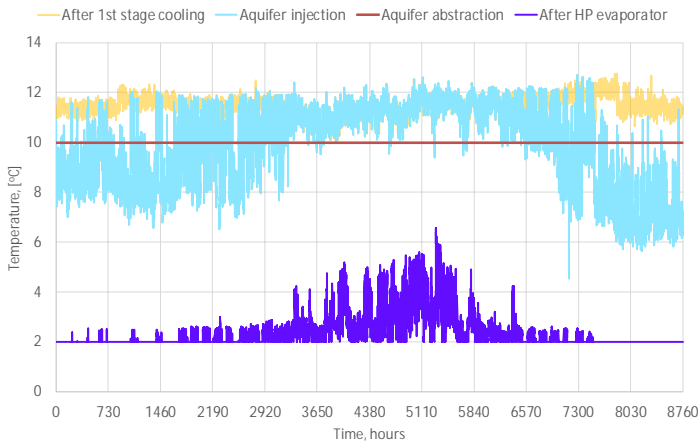


Figure 5. Annual evolution of ATES temperatures (Sc.2)

Impact on groundwater areas

Although the undisturbed aquifer temperature is as high as 10 °C, first stage cooling can be used 8736 out of 8760 hours annually, and it represents 17% of the cooling demand covered by GSHP (some 1,6 out of 9.6 GWh). This configuration also increases the temperature before GSHP evaporator by 1.5 °C on average, which improves the COP and enhances heat pump's capacity in the evaporator as well. The average injection temperature lays in a narrow range of roughly 10 ± 1 °C, which justifies a one-way ATES operation and consequently, the thermal impact on the aquifer remains very limited.

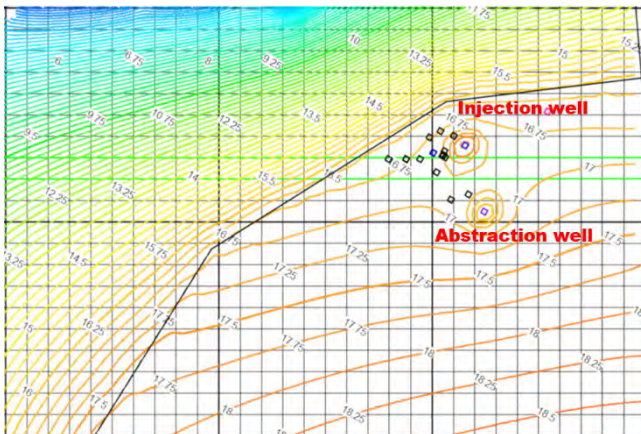


Figure 6. Hydraulic impact after 20 years (Sc. 2)

The long-term hydraulic impact is simulated in ModelMuse and the result after 20 years of one-way operation is presented in Figure 6, where hydraulic head is represented by the iso-lines with resolution of 0.25m. In order to mitigate the hydraulic impact of ATES pumping, the injection well is placed downstream while abstraction well is located upstream (Figure 6). The maximum simulated drawdown is 1.25 m, which corresponds to 4.9 m inside the pumping well. The overall impact of ATES pumping vanishes in about 500 m from each well, thus it is not affecting in significant way the surrounding groundwater areas.

Conclusion

The presented case study was successful in demonstrating and developing a mathematical model for system's management: calculation of GSHP recirculation flow, estimation of heat pump COP, as well as an algorithm for computation of ATES pumping flow rate based on the capacity to cover heating and cooling demand in a single process. Additionally, system's technoeconomic feasibility, efficiency and the impact of GSHP-ATES operation on the nearby aquifer were evaluated. Groundwater model was developed and calibrated, utilizing different available data sources like the National Land Survey of Finland, Finnish Environment Institute and Geological Survey of Finland, as well as computational and modelling tools like MS Excel, QGIS and ModelMuse (MODFLOW).

The dispatch of combined heating and cooling loads using annual data of existing Finnish urban district was used in tandem with GSHP-ATES model. It presented attractive economic outcome – competitive energy production cost around 30 €/MWh, far below 79.11 €/MWh, which is the weighted average DH price in Finland (DH, 2018), as well as very limited long-term impact on the nearby aquifer. The maximum drawdown within the pumping well was estimated as 4.9 m after 20 years of operation, and the overall hydraulic impact is limited to 500 m around the wells. Injection temperature deviates from undisturbed aquifer temperature by roughly ± 1 °C on average, fulfilling the International legislation regarding groundwater temperature thresholds (Haehnlein et al. 2010). The future transition to low district heating networks (Guzzini et al. 2020) by the introduction of GSHP, can eventually benefit from the proposed mathematical methodology due to its capability to find a trade-off between the energy production cost, ATES pumping flow rate and the temperature drop introduced by the heat pump in DH supply line. Moreover, a sensitivity analysis of system's operation has been performed by Todorov et al. (2020b), showing how exponent parameter p influences the energy production cost, the induced temperature drop in DH supply as well as the overall performance of GSHP (COP).

Overall, ATES-GSHP tandem results to be a sustainable and effective alternative to the conventional thermal energy generation primarily based on fossil fuels. It is acknowledged the efficiency of ATES-GSHP systems due to their ability to recycle heating & cooling loads, using the subsurface as thermal storage within integrated district energy networks, especially in urban areas. Last but not least: air pollution in cities, responsible for many chronic & acute illness and premature deaths, can be effectively mitigated by the introduction of greener energy technologies and gradually eliminating the utilization of fossil fuels.

Acknowledgments

The present work was carried out as part of the Smart Otaniemi project (Aalto University) and was funded by Business Finland. We wish to thank Global Eco Solutions – Finland, for their valuable support within the GESATES project.

Nomenclature

Φ	[W]	Heating/cooling loads
h	[m]	Hydraulic head
K	[m/s]	Hydraulic conductivity
k	[-]	Power fraction HP/demanded DH load
P	[W]	Power demand (pumping)
p	[-]	Exponent parameter
Q	[m ³ /s]	Pumping flow rate
R	[m/s]	Aquifer recharge
S	[-]	Aquifer storativity
$S_{VC,wat}$	[J/m ³ K]	Water volumetric heat capacity
$T_{DH,S}$	[°C]	DH supply temperature
$T_{DH,R}$	[°C]	DH return temperature
$T_{DC,S}$	[°C]	DC supply temperature
$T_{DC,R}$	[°C]	DC return temperature
$T_{HPC,S}$	[°C]	HP condenser supply temperature
$T_{HPC,R}$	[°C]	HP condenser return temperature
$T_{HPE,I}$	[°C]	HP evaporator inlet temperature
$T_{HPE,O}$	[°C]	HP evaporator outlet temperature
$T_{lm,H}$	[°C]	Sink logarithmic mean temperature
$T_{lm,L}$	[°C]	Source logarithmic mean temperature
ΔT_{DH}	[°C]	DH supply / return temp. difference
ΔT_{HPC}	[°C]	Temperature difference HP condenser
ΔT_{DHS}	[°C]	Temp. drop in DH supply after HP

References

- Arola, T. & Korkka-Niemi, K. (2014). The effect of urban heat islands on geothermal potential: Examples from Quaternary aquifers in Finland. *Hydrogeology Journal*, 22(8), pp. 1953-1967. <https://doi.org/10.1007/s10040-014-1174-5>
- Bayer, P., Attard, G., Blum, P., & Menberg, K. (2019). The geothermal potential of cities. *Renewable and Sustainable Energy Reviews*. <https://doi.org/10.1016/j.rser.2019.02.019>
- DAE 2020, Danish Energy Agency, Technology Data for Generation of Electricity and District Heating (accessed 17.2.2020) <https://ens.dk/en/our-services/projections-and-models/technology-data/technology-data-generation-electricity-and>
- DH 2008, Guidelines for District Heating Substations, Approved by the Euroheat & Power Board, Prepared by Task Force Customer Installations (accessed 12.2.2020): <https://www.euroheat.org/wp-content/uploads/2008/04/Euroheat-Power-Guidelines-District-Heating-Substations-2008.pdf>
- DH 2018. Finnish Energy, District Heating in Finland 2018. Available online (accessed 22.7.2020): https://energia.fi/files/4092/District_heating_in_Finland_2018.pdf
- Drenkelfort, G., Kieseler, S., Pasemann, A., & Behrendt, F. (2015). Aquifer thermal energy storages as a cooling option for German data centers. *Energy Efficiency*, pp. 385–402. <https://doi.org/10.1007/s12053-014-9295-1>
- Eurostat 2020: Renewable energy for heating and cooling (accessed 21.2.2020) <https://ec.europa.eu/eurostat/web/products-eurostat-news/-/DDN-20200211-1?inheritRedirect=true&redirect=%2Feurostat%2F>
- Fleuchaus, P., Godschalk, B., Stober, I., & Blum, P. (2018). Worldwide application of aquifer thermal energy storage – A review. *Renewable and Sustainable Energy Reviews*, pp. 861-876. <https://doi.org/10.1016/j.rser.2018.06.057>
- Fleuchaus, P. et al. (2020) Performance analysis of Aquifer Thermal Energy Storage (ATES), *Renewable Energy*, Volume 146, Pages 1536-1548, ISSN 0960-1481, <https://doi.org/10.1016/j.renene.2019.07.030>
- Greenpeace 2020: Toxic air: The price of fossil fuels, February 2020, (accessed 4.5.2020): <https://www.greenpeace.org/usa/wp-content/uploads/2020/02/The-Price-of-Fossil-Fuels-media-briefing.pdf>
- Grundfos NB/NBG centrifugal pumps: <https://www.grundfos.com/products/find-product/nb-nbg-nbe-nbge.html> (accessed 17.2.2020)
- Grundfos SP submersible pumps: <https://www.grundfos.com/products/find-product/sp.html> (accessed 17.2.2020)
- Guzzini, Alessandro & Pellegrini, Marco & Pelliconi, Edoardo & Saccani, and. (2020). Low Temperature District Heating: An Expert Opinion Survey. *Energies*. <https://doi.org/10.3390/en13040810>
- Haehnlein, S., Bayer, P., & Blum, P. (2010). International legal status of the use of shallow geothermal energy. *Renewable and Sustainable Energy Reviews*, pp. 2611-2625. <https://doi.org/10.1016/j.rser.2010.07.069>
- Harbaugh, Arlen, W. (2005). MODFLOW-2005, The U. S. Geological Survey Modular Ground-Water Model — the Ground-Water Flow Process. *U.S. Geological Survey Techniques and Methods 6-A15*. <https://doi.org/10.3133/tm6A16>
- Joronen, L. (2009) Groundwater protection plan for Turku, Kaarina and Rusko orig. title "Turun, Kaarinan ja Ruskon pohjavesialueiden suojelusuunnitelma":

- https://www.turku.fi/sites/default/files/atoms/files/2010-turun_kaarinan_ja_ruskon_pohjavesialueiden_suojelusuunnitelma.pdf (accessed 10.2.2020)
- Luoma, S. (2018) Groundwater flow models of the shallow aquifer in Hanko (accessed 10.2.2020) http://tupa.gtk.fi/raportti/arkisto/95_2018.pdf
- ModelMuse: A Graphical User Interface for Groundwater Models: <https://www.usgs.gov/software/modelmuse-a-graphical-user-interface-groundwater-models> (accessed 13.3.2020)
- Nielsen, S., & Möller, B. (2013). GIS based analysis of future district heating potential in Denmark. *Energy*, pp. 458-468. <https://doi.org/10.1016/j.energy.2013.05.041>
- Nordpool Finnish monthly prices 2006-2020 (accessed 12.3.2020): <https://www.nordpoolgroup.com/Market-data/Dayahead/Area-Prices/FI/Monthly/?dd=FI&view=table>
- Paiho, S., Saastamoinen, H., Hakkarainen, E., Similä, L., Pasonen, R., Ikäheimo, J., Horsmanheimo, S. (2018). Increasing flexibility of Finnish energy systems—A review of potential technologies and means. *Sustainable Cities and Society*. <https://doi.org/10.1016/j.scs.2018.09.015>
- Pellegrini, M., Bloemendal, M., Hoekstra, N., Spaak, G., Andreu Gallego, A., Rodriguez Comins, J., Steeman, H. (2019). Low carbon heating and cooling by combining various technologies with Aquifer Thermal Energy Storage. *Science of the Total Environment*, pp. 1-10. <https://doi.org/10.1016/j.scitotenv.2019.01.135>
- Popovski, E., Aydemir, A., Fleiter, T., Bellstädt, D., Büchele, R. & Steinbach, J. (2019). The role and costs of large-scale heat pumps in decarbonising existing district heating networks – A case study for the city of Herten in Germany. *Energy*, 180, pp. 918-933. <https://doi.org/10.1016/j.energy.2019.05.122>
- QGIS - A Free and Open Source Geographic Information System: <https://www.qgis.org/en/site/> (accessed 13.3.2020)
- Reinholdt, L., Kristófersson, J., Zühlendorf, B., Elmegaard, B., Jensen, J., Ommen, T. & Jørgensen, P. (2018). Heat pump COP, part 1: Generalized method for screening of system integration potentials. *Refrigeration Science and Technology*, 2018-, pp. 1207-1213. <https://doi.org/10.18462/iir.gl.2018.1380>
- Schmidt, T., Pauschinger, T., Sørensen, P.A., Snijders, A., Thornton, J. (2018) Design Aspects for Large-scale Pit and Aquifer Thermal Energy Storage for District Heating and Cooling. *Energy Procedia*, Volume 149, September 2018, Pages 585-594. <https://doi.org/10.1016/j.egypro.2018.08.223>
- Schüppler, S., Fleuchaus, P., & Blum, P. (2019). Techno-economic and environmental analysis of an Aquifer Thermal Energy Storage (ATES) in Germany. *Geothermal Energy*. <https://doi.org/10.1186/s40517-019-0127-6>
- Soltani, M., M. Kashkooli, F., Dehghani-Sanij, A., Kazemi, A., Bordbar, N., Farshchi, M., . . . B. Dusseault, M. (2019). A comprehensive study of geothermal heating and cooling systems. *Sustainable Cities and Society*, 44, pp. 793-818. <https://doi.org/10.1016/j.scs.2018.09.036>
- Todorov, O., Alanne, K., Virtanen, M. & Kosonen, R. (2020a). A method and analysis of aquifer thermal energy storage (ATES) system for district heating and cooling: A case study in Finland. *Sustainable Cities and Society*, 53. <https://doi.org/10.1016/j.scs.2019.101977>
- Todorov, O., Alanne, K., Virtanen, M. & Kosonen, R. (2020b). Aquifer Thermal Energy Storage (ATES) for District Heating and Cooling: A Novel Modeling Approach Applied in a Case Study of a Finnish Urban District. *Energies*, 13(10), p. 2478. <https://doi:10.3390/en13102478>
- Wu, X., Nethery, R. C., Sabath, B. M., Braun, D., & Dominici, F. (2020). Exposure to air pollution and COVID-19 mortality in the United States. *MedRxiv*. <https://doi.org/10.1101/2020.04.05.20054502>